Quasi-Two-Dimensional Mott Transition System $Ca_{2-x}Sr_xRuO_4$

S. Nakatsuji[1] and Y. Maeno[1,2]

[1]*Department of Physics, Kyoto University, Kyoto 606-8502, Japan*

[2]*CREST, Japan Science and Technology Corporation, Kawaguchi, Saitama 332-0012, Japan*

(Received 28 December 1998)

We have revealed the phase diagram of $Ca_{2-x}Sr_xRuO_4$: the quasi-two-dimensional Mott transition system that connects the Mott insulator Ca_2RuO_4 with the spin-triplet superconductor Sr_2RuO_4. Adjacent to the metal/nonmetal transition at $x \simeq 0.2$, we found an antiferromagnetically correlated metallic region where non-Fermi-liquid behavior in resistivity is observed. Besides this, the critical enhancement of susceptibility toward the region boundary at $x_c \simeq 0.5$ suggests the crossover of magnetic correlation to a nearly ferromagnetic state, which evolves into the spin-triplet superconductor Sr_2RuO_4.

PACS numbers: 71.30.+h, 74.70.–b, 75.40.–s

Much attention has been paid to the quasi-two-dimensional Mott transition systems, such as high-T_c cuprates and organic conductors, for their dramatic variation of the electronic states between the extremes of ground states: insulating state and superconductivity. Particularly, the mechanism of the emergence of the unconventional superconductivity from the Mott insulator has been one of the main focuses of intense investigation. Intriguing links have also been revealed between anomalous metallic states near the metal-insulator transition and non-Fermi-liquid (NFL) behavior in the quantum critical regime of a number of heavy fermion compounds [1].

While the d-wave pairing has been revealed in the cuprates, the p-wave superconductivity in Sr_2RuO_4, which is isostructural to one of the best studied cuprates $La_{2-x}Sr_xCuO_4$, has attracted recent interest [2–4]. The spin-triplet pairing in Sr_2RuO_4 has been demonstrated by NMR Knight shift measurement [3]. As expected from the exotic pairing, its normal state is a highly correlated metal, well described as a quasi-two-dimensional Fermi liquid [5,6]. In contrast, isovalent Ca substitution for Sr drastically changes this superconductor into the Mott insulator Ca_2RuO_4 [7,8]. The decrease of $4d$-band width in comparison with that of Sr_2RuO_4, caused by distortions in RuO_2 planes, leads to a Mott-Hubbard-type gap [7,9,10]. Therefore, the new solution system $Ca_{2-x}Sr_xRuO_4$ should provide the important information on the Mott transition route that involves the emergence of the spin-triplet superconductor.

In this Letter, we present the first results on the phase diagram of the quasi-two-dimensional Mott transition system $Ca_{2-x}Sr_xRuO_4$. The metal/nonmetal (M/NM) transition occurs in the Ca-rich region by varying either the Sr content or the temperature. On the verge of the M/NM transition at $x \simeq 0.2$, we have found an antiferromagnetically (AF) correlated metallic region where non-Fermi-liquid behavior in resistivity has been observed. Furthermore, toward the region boundary at $x_c \simeq 0.5$, the system reveals the critical enhancement of low temperature susceptibility. This suggests the crossover of magnetic correlation to a nearly ferromagnetic (FM) state, which evolves into the spin-triplet superconductor with enhanced paramagnetism.

We have recently succeeded in synthesizing polycrystalline $Ca_{2-x}Sr_xRuO_4$ in the whole region of x, and in growing single crystals by a floating-zone method in the region $0.0 \leq x \leq 0.7$, in addition to Sr_2RuO_4 ($x = 2$). Details of the preparations will be described elsewhere [11]. The crystal structures are studied by powder x-ray diffraction at room temperature. While Ca_2RuO_4 has an orthorhombic Pbca symmetry [9], all the other spectra of $Ca_{2-x}Sr_xRuO_4$ show only the peaks that are well indexed with the single pseudotetragonal symmetry, consistent with I4/mmm of Sr_2RuO_4. Determination of their precise symmetries is under investigation [12]. Here we adopt the notations for the unit cell with I4/mmm symmetry. Electrical resistivity was measured down to 4.2 K by a standard four-probe dc method and down to 0.3 K by an ac method. Magnetization measurements down to 1.8 K were performed with a SQUID magnetometer.

We have determined the phase diagram as represented in Fig. 1, which consists of the following three regions:

(I) ($0 \leq x < 0.2$) AF insulating ground state. M/NM transition occurs by varying temperature except $x = 0$. Ca_2RuO_4 ($x = 0$) is an insulator at least up to 300 K. M/NM transition by varying x occurs at $x \simeq 0.2$.

(II) ($0.2 \leq x < 0.5$) "Magnetic metallic (M-M) region" below the peak temperature T_P of the susceptibility.

(III) ($0.5 \leq x \leq 2$) Paramagnetic metal. Low temperature susceptibility exhibits critical enhancement at $x_c \simeq 0.5$. Superconductivity with $T_c = 1.5$ K at $x = 2$.

In the paragraphs below, we will describe these characteristic properties of each region in the order of regions I, II, and III. Finally, the physical origin of this distinct variation of the ground state will be discussed.

First, we summarize in Fig. 2 the temperature dependence of the in-plane resistivity $\rho_{ab}(T)$ measured on cooling for various values of x. In region I, $\rho_{ab}(T)$ of the stoichiometric Ca_2RuO_4 ($x = 0$) basically shows activation-type insulating behavior with an activation energy of 0.2 eV [13]. Besides, the electronic specific-heat coefficient was found to be 0 ± 0.2 mJ/mol K^2,

 0031-9007/00/84(12)/2666(4)$15.00

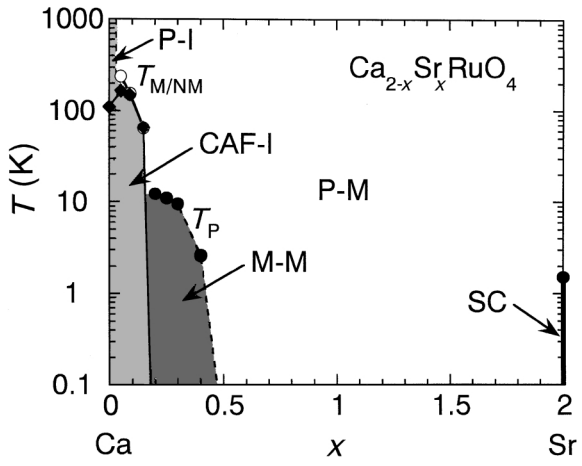

FIG. 1. Phase diagram of $Ca_{2-x}Sr_xRuO_4$ with the abbreviations: P for paramagnetic, CAF for canted antiferromagnetic, M for magnetic, SC for superconducting phase, -M for metallic phase, and -I for insulating phase. The solid circle, the open circle, and the solid diamond represent the peak temperature T_P of the susceptibility for the [001] component, the metal/nonmetal transition temperature $T_{M/NM}$, and the CAF transition temperature T_{CAF}, respectively.

which manifests that Ca_2RuO_4 is truly an insulator with no density of states at the Fermi level $N(E_F)$ [13].

In contrast, slight Sr substitution for Ca stabilizes a metallic state at high temperatures, and induces the M/NM transition at a temperature $T_{M/NM}$ on cooling as in Fig. 1. The results of $x = 0.09$ and 0.15 in Fig. 2 represent $\rho_{ab}(T)$ for region I with $T_{M/NM} \simeq 155$ and 70 K, respectively. With abrupt increases by factors more than 10^4 at $T_{M/NM}$, they show the nonmetallic behavior described by variable-range hopping. For $x = 0.15$, for example, the data below $T_{M/NM}$ well fit $\rho_{ab}(T) = A\exp(T_0/T)^{1/4}$ with $T_0 = 9 \times 10^4$ K. This suggests that strong localization dominating the nonmetallic behavior drives the M/NM transition, preceding the gap opening toward the Mott insulator. Below $T_{M/NM}$, the susceptibility χ also shows a distinct magnetic transition at a temperature T_{CAF} on cooling, which finally coincides with the M/NM transition for about $x \geq 0.1$. The magnetization vs the field (M-H curve) at 5 K exhibits weak FM hysteresis ascribable to canted AF as in Ca_2RuO_4 [7,9]. The M/NM transition of the ground state occurs at $x \simeq 0.2$, as illustrated in Fig. 2.

Powder neutron diffraction measurements have been carried out for $x = 0.1$ and 0.2 down to 1.5 K [12], and shown that the M/NM transition either by varying x or T involves the first-order structural transition, consistent with the thermal hystereses observed in $\rho(T)$ and $\chi(T)$.

What characterizes the M-M region in region II is the susceptibility peak. Figure 3 shows $\chi(T)$ curves for $x = 0.2$ under fields of 1 T parallel to [110], [1$\bar{1}$0], and [001] axes. The in-plane susceptibility exhibits the maximum and the minimum for fields along [110] and [1$\bar{1}$0], respectively. There is no observable difference between field-cooled and zero-field-cooled data, so our measurements are not suggestive of spin glass ordering. The most prominent feature is the broad maximum in each axis component. Well above T_P, these components show Curie-Weiss (C-W) behavior with AF Weiss temperatures Θ_W comparable to T_P. Such characteristics indicate that some kind of AF ordering occurs at T_P.

However, the broad nature of these maxima is far from the usual sharp cusp at a Néel point. Moreover, the peak temperatures T_P for the in-plane components are definitely different from each other: $T_P^{[110]}$ for the easy-axis [110] is 8.2 K, while $T_P^{[1\bar{1}0]}$ for the hard-axis [1$\bar{1}$0] is 12.2 K, identical to that for the c-axis [001]. Therefore, although the substantial reduction of the susceptibility should originate from the AF correlation, the long-range order (LRO) does not emerge at T_P, but is somehow destabilized. In fact, no magnetic LRO with a moment larger than the resolution limit of 0.05 μ_B was detected for $x = 0.2$ down to 1.5 K in the neutron diffraction measurement [12].

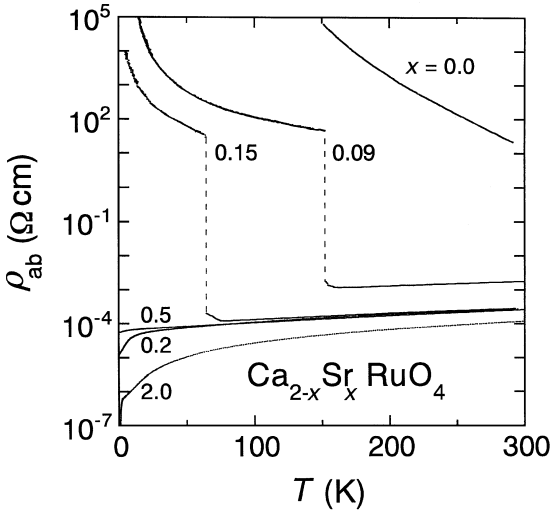

FIG. 2. Temperature dependence of the in-plane resistivity $\rho_{ab}(T)$ for $Ca_{2-x}Sr_xRuO_4$ with different values of x. The vertical broken lines are guides to the eye.

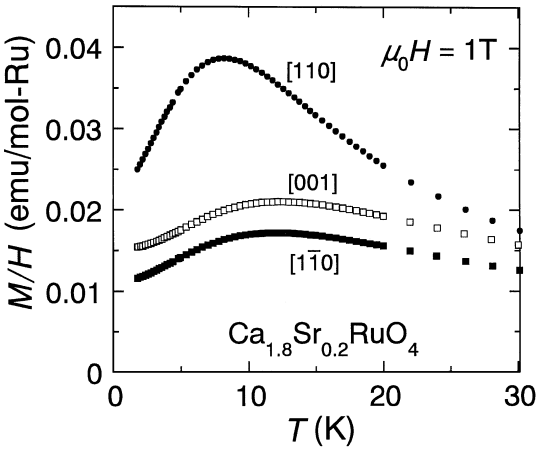

FIG. 3. Temperature dependence of the susceptibility of $Ca_{1.8}Sr_{0.2}RuO_4$ under $\mu_0H = 1$ T parallel to each axis. Field-cooled and zero-field-cooled curves agree very well.

Another evidence for the AF correlation in the M-M region is the anisotropy of the susceptibility below T_P. As shown in Fig. 3, the [110] component decreases on cooling almost 3 times more than the others. This corresponds to the anisotropy for an AF ordering with the easy-axis [110] and with the hard-axes $[1\bar{1}0]$ and [001]. In fact, the anisotropy obtained here is very similar to that of the AF-LRO state in Ca_2RuO_4 [13], with spins aligned antiferromagnetically along the [110] axis [9]. Moreover, the *M-H* curve in this region exhibits a metamagnetic transition (for example, at $\mu_0 H \approx 2.5$ T $\|$ [110] for $x = 0.2$), similar to the one observed in the ordered Ca_2RuO_4 [8]. These substantial resemblances indicate that an AF short-range order (AF-SRO) is well stabilized in the magnetic *metallic* region just next to the M/NM transition.

As presented in Fig. 4, the most intriguing systematic variation in the *metallic* regions II and III was found in the low temperature susceptibility $\chi(0)$, represented here by the value at 2 K. The inset of Fig. 4 displays $\chi(T)$ curves for region III under a field of 0.1 T parallel to the *ab* plane. The in-plane susceptibility is almost isotropic in this region. For Sr_2RuO_4, the $\chi(T)$ curve is Pauli-paramagnetic for its Fermi liquid state. The Ca substitution, however, continuously changes it to C-W–like, and finally to Curie-like with $\Theta_W \simeq 0$ K at $x = 0.5$. Corresponding to this evolution of the C-W behavior, $\chi(0)$ for $2.0 \geq x \geq 0.5$ in Fig. 4 increases with decreasing x. It is critically enhanced at $x = 0.5$, reaching a value more than 100 times larger than that of Sr_2RuO_4.

The enhancement is consistent with the expected increase in $N(E_F)$ by the band narrowing with the Ca substitution. However, this effect alone cannot explain the strong temperature dependence near $x = 0.5$. In an itinerant system like this, such an increase of negative Θ_W to zero is ascribable to the evolution of FM spin fluctuations [14]. Therefore, with the enlarged $N(E_F)$, it should be the Stoner enhancement that plays a significant role in the critical behavior around $x = 0.5$. In region II, on the other hand, $\chi(0)$ sharply decreases with decreasing x, reflecting the formation of the susceptibility peak at the higher temperature T_P as shown in Fig. 1.

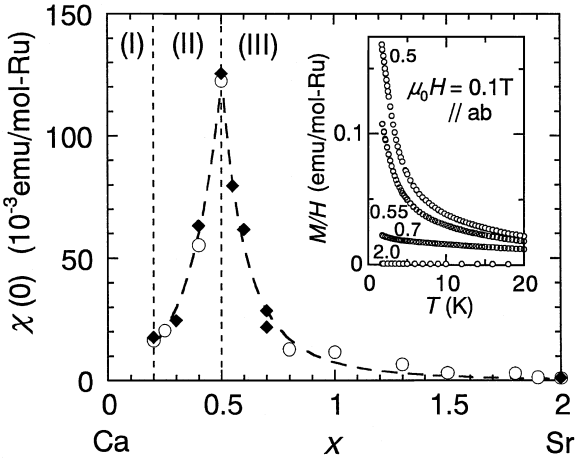

FIG. 4. $\chi(0)$: the susceptibility at 2.0 K against the Sr concentration x in the metallic regions II and III. The values for the polycrystalline samples are indicated by open circles, while for the single crystals, the solid diamonds represent the mean values $\chi_m(0)$ determined by the relation: $\chi_m(0) = \{\chi_a(0) + \chi_b(0) + \chi_c(0)\}/3$. The broken lines are guides to the eye. The inset displays $\chi(T)$ curves for region III under a field of 0.1 T parallel to the *ab* plane. Field-cooled and zero-field-cooled curves agree very well.

We note that this critical enhancement of $\chi(0)$ occurs at $x = 0.5$, and thus appears to be correlated with Θ_W approaching zero in region III and T_P increasing from zero in region II. This criticality indicates a drastic change of the ground state at the M-M region boundary, most likely from the nearly FM state to the AF correlated one. Since we detected no evidence of magnetic LRO down to 0.3 K, it should be a magnetic crossover that occurs at $x_c \simeq 0.5$. Quite recently, however, a preliminary neutron diffraction measurement has found a second-order structural transition in region II from a high temperature tetragonal to a low temperature orthorhombic phase [12]. It is also at x_c that the transition temperature emerges from zero, just as T_P, while it increases much more rapidly than T_P with decreasing x. This coincidence strongly implies that the structural transition induces the magnetic crossover.

The low temperature parts of $\rho_{ab}(T)$ in Fig. 2 for $x = 0.2$, 0.5, and 2 are presented in Fig. 5, where $\rho_{ab}(T) - \rho_{ab}(0)$ is plotted against $T^{1.4}$. Sr_2RuO_4 shows T-squared dependence as indicated by a fitting curve, reflecting its Fermi liquid state established by a variety of measurements [5,6]. In contrast, for $x = 0.2$ and 0.5, the in-plane resistivities severely deviate from the T-squared dependence. The best fit was obtained in the form of $\rho_{ab}(T) = \rho_{ab}(0) + AT^{1.4}$. At $x = 0.5$, this $T^{1.4}$ dependence appears below about 3 K following the T-linear one up to 5.5 K. Meanwhile, the resistivity for $x = 0.2$ starts to decrease strongly below about $T_P^{[110]} \approx 8$ K and shows the $T^{1.4}$ dependence toward the lowest temperature.

Work on heavy fermion compounds and cuprates has revealed that such NFL behavior is due to critical fluctuations, and persists to low temperature near a magnetic instability [1,15]. Therefore, the NFL behavior observed down to 0.3 K not only around $x_c \simeq 0.5$ but at $x = 0.2$ suggests that the enhanced spin fluctuations, which destabilize the magnetic LRO, dominate the entire M-M region. In a two-dimensional system near AF and FM instabilities, the resistivity is expected to show T-linear [16] and $T^{4/3}$ [17] dependence, respectively. The observed $T^{1.4}$ dependence is quite close to the latter one, which is also found in Sr_2RuO_4 under pressure [18]. Along with the strong enhancement of the low temperature susceptibility, this gives a consistent interpretation that $x_c \simeq 0.5$ is just near a FM instability. On the other hand, for the AF-SRO in the M-M region, there are basically two possible spin configurations: simple in-plane AF or interlayer AF with the dominant in-plane FM spin fluctuations. It is not possible to distinguish between these possibilities on the basis

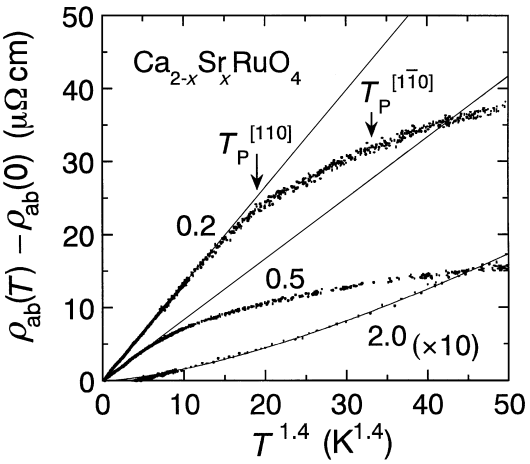

FIG. 5. Temperature dependence of the in-plane resistivity $\rho_{ab}(T)$ for $x = 0.2$, 0.5, and 2. Solid lines indicate fits with T^2 ($x = 2$), and $T^{1.4}$ ($x = 0.2$ and 0.5) dependence. The peak temperatures of the susceptibilities are indicated for $x = 0.2$.

of the current data. Further studies by neutron diffuse scattering are needed for this region.

In Fig. 5, it should also be noted that $\rho_{ab}(T) - \rho_{ab}(0)$ becomes smaller with x. This most probably results from the weakened inelastic (especially, spin) scattering due to the band widening. Moreover, for $x = 0.2$, the formation of AF-SRO should induce the strong decrease in $\rho_{ab}(T)$ (below T_P) because of the reduced spin scattering. In fact, well below T_P, the field dependence of the longitudinal in-plane magnetoresistance ($I \parallel H \parallel$ ab) for $x = 0.2$ shows a clear peak at $\mu_0 H \approx 2.8$ T, corresponding to the metamagnetic transition, while only a negative dependence was observed above T_P [11]. Nevertheless, the residual resistivity $\rho_{ab}(0)$ for $x = 0.2$ is smaller than that for $x = 0.5$, as in Fig. 2. Since $\rho_{ab}(0)$ is basically determined by the imputity scattering [19], this is attributable to the less randomness in Ca/Sr distribution at $x = 0.2$.

Finally, let us discuss the physical origin of the distinct variation of the ground state in this system. Recent NMR studies clarified that the magnetic interaction in Sr_2RuO_4 is characterized by the weakly ferromagnetic spin fluctuations with the exchange-enhanced in-plane susceptibility [20,21]. This suggests that local spins in triply degenerate t_{2g} orbitals are coupled ferromagnetically with each other. In contrast with the half-filled case, the addition of the fourth electron will align spins at neighboring sites through Hund's coupling, thereby gaining kinetic energy against Coulomb repulsion. This local ferromagnetic interaction must be crucial for the spin-triplet pairing. Nevertheless, as in Fig. 1, Sr_2RuO_4 at $x = 2$ is the singular point for this superconductivity, which disappears already at $x = 1.95$, probably owing to the disorder intrinsic to the Ca substitution.

In contrast with undistorted Sr_2RuO_4, the RuO_2 plane in Ca_2RuO_4 is so severely distorted that RuO_6 octahedra have unusually flattened shape along the interlayer direction through the Jahn-Teller effect [9]. Thus, the three t_{2g} orbitals originally degenerate in Sr_2RuO_4 will split into d_{xy} with lower energy and the almost degenerate d_{yz} and d_{zx} with higher energy. Filling them with four electrons, Ca_2RuO_4 may well have the half-filled band, which favors the Mott insulating ground state with AF superexchange coupling between neighboring spins.

Connecting these opposite ground states of the end members, the nearly FM state evolved from Sr_2RuO_4 through band narrowing, starts to change into the AF correlated one beyond $x_c \simeq 0.5$. The orbital rearrangement involved in the structural symmetry change may probably cause such a crossover of magnetic correlation. Consequently, not only the band-width control by the Ca/Sr substitution, but the control of the effective filling of carriers through the orbital degeneracy tuning (which may be called "k-space doping") must be essential in this Mott transition system $Ca_{2-x}Sr_xRuO_4$, in contrast with the high-T_c cuprates with a single $d_{x^2-y^2}$ orbital.

The authors acknowledge T. Ishiguro for his support and M. Braden for important collaboration, especially for allowing us to use unpublished information. They are grateful to H. Fukazawa, M. Minakata, and S. Ikeda for their technical support and valuable discussions, to A. P. Mackenzie, K. Yamada, H. Fukuyama, and K. Ishida for useful discussions. This work has been supported in part by a Grant-in-Aid for Scientific Research from the Ministry of Education, Science, Sports and Culture of Japan. One of the authors (S. N.) has been supported by JSPS.

[1] See, for example, J. Phys. Condens. Matter **8** (1996).
[2] Y. Maeno *et al.,* Nature (London) **372**, 532 (1994).
[3] K. Ishida *et al.,* Nature (London) **396**, 658 (1998). Since the sample is in the clean limit with a mean free path ≈500 nm, the invariance of the Knight shift across T_c cannot be attributed to the spin-orbit scattering mechanism in the dirty spin-singlet superconductor.
[4] G. M. Luke *et al.,* Nature (London) **394**, 558 (1998).
[5] A. P. Mackenzie *et al.,* Phys. Rev. Lett. **76**, 3786 (1996).
[6] Y. Maeno *et al.,* J. Phys. Soc. Jpn. **66**, 1405 (1997).
[7] S. Nakatsuji *et al.,* J. Phys. Soc. Jpn. **66**, 1868 (1997).
[8] G. Cao *et al.,* Phys. Rev. B **56**, R2916 (1997).
[9] M. Braden *et al.,* Phys. Rev. B **58**, 847 (1998).
[10] A. V. Puchkov *et al.,* Phys. Rev. Lett. **81**, 2747 (1998).
[11] S. Nakatsuji *et al.* (unpublished).
[12] M. Braden (private communication).
[13] H. Fukazawa *et al.* (to be published).
[14] T. Moriya, *Spin Fluctuations in Itinerant Electron Magnetism* (Springer, Berlin, 1985).
[15] A. J. Millis, Phys. Rev. B **48**, 7183 (1993).
[16] For example, T. Moriya *et al.,* J. Phys. Soc. Jpn. **59**, 2905 (1990).
[17] M. Hatatani *et al.,* J. Phys. Soc. Jpn. **64**, 3434 (1995).
[18] K. Yoshida *et al.,* Phys. Rev. B **58**, 15 062 (1998).
[19] T. M. Rice *et al.,* Phys. Rev. B **5**, 4350 (1972).
[20] H. Mukuda *et al.,* J. Phys. Soc. Jpn. **67**, 3945 (1998).
[21] T. Imai *et al.,* Phys. Rev. Lett. **81**, 3006 (1998).